ORIGINAL PAPER

Synthesis and Properties of Diphenylcarbazole Triphenylethylene Derivatives with Aggregation-Induced Emission, Blue Light Emission and High Thermal Stability

Bing-jia Xu · Zhen-guo Chi · Xiao-fang Li · Hai-yin Li · Wei Zhou · Xi-qi Zhang · Cheng-cheng Wang · Yi Zhang · Si-wei Liu · Jia-rui Xu

Abstract New aggregation-induced emission materials derived from diphenylcarbazole triphenylethylene were prepared. The thermal, photophysical, electrochemical and aggregation-induced emissive properties were investigated. All the compounds had strong blue light emission capability and excellent thermal stability. Their maximum fluorescence emission wavelengths were between 450 to 460 nm in TLC plates, while their glass transition temperatures ranged from 162.2 to 182.4 °C. The decomposition temperatures of the synthesized compounds were all well over 500 °C. The synthesized compounds possessed aggregation-induced emission (AIE) properties, which exhibited enhanced fluorescence emissions in aggregation states or in solid states. The HOMO energy levels estimated from the oxidation potentials were found in the range from 5.49 to 5.52 eV. The lowest unoccupied molecular orbital/highest occupied molecular orbital (LUMO/HOMO) energy gaps (ΔE_g) for the compounds were estimated from the onset absorption wavelengths of UV absorption spectra and ranged from 3.04 to 3.20 eV.

Keywords Triphenylethylene · Blue light emission · High thermal stability · Synthesis · Aggregation-induced emission

B.-j. Xu · Z.-g. Chi (✉) · X.-f. Li · H.-y. Li · W. Zhou · X.-q. Zhang · C.-c. Wang · Y. Zhang · S.-w. Liu · J.-r. Xu (✉)
PCFM Lab, DSAPM Lab, FCM Institute,
State Key Laboratory of Optoelectronic Materials and Technologies,
School of Chemistry and Chemical Engineering,
Sun Yat-sen University,
Guangzhou 510275, China
e-mail: chizhg@mail.sysu.edu.cn

J.-r. Xu
e-mail: xjr@mail.sysu.edu.cn

Introduction

Most luminescent materials, such as thin films of organic light-emitting diodes [1–5], are used in the solid state. However, the efficiency of solid-state luminescent materials is unsatisfactory due to quenching caused by aggregation. This quenching is due mainly to both strong π–π stacking interactions and non-radiative decay [6–9], thereby hindering many scientists from finding luminescent materials that could be used in a wide variety of applications.

Recently, several types of electroluminescent materials, including siloles and 1-cyanotrans-1,2-bis-(4-methylbiphenyl) ethylene, were found by Tang and Park to possess abnormal luminescent properties, in which light emission is enhanced from an aggregated or solid state [10–14]. This interesting luminescent property has been named aggregation-induced emission (AIE) [10] or aggregation-induced emission enhancement (AIEE) [11]. Currently, more and more AIE materials have been found, such as tetraphenylethene (TPE) derivatives, among others, for potential application as active layers in organic light emitting diodes (OLEDs) or fluorescent diagnostic kits [15–17].

Triphenylethylene carbazole derivatives, a new kind of AIE-active molecules with excellent thermal properties and blue light emission capabilities, were first found in our laboratory. The twisted configuration of triphenylethylene, the core of the derivative, is assumed to have made it AIE active and that the functional groups around triphenyl-ethylene enhanced this phenomenon [18].

Further research on the triphenylethylene system was performed by our team. As a result, diphenylcarbazole triphenylethylene derivatives, which are AIE active and have much better thermal properties as well as stronger blue light emission, were successfully synthesized.

Experimental

Materials and Methods

All reagents and chemicals purchased from Alfa Aesar were used as received. Tetrahydrofuran (THF) was distilled from sodium/benzophenone. Ultra-pure water was used in the experiments. All other solvents were purchased as analytical grade from Guangzhou Dongzheng Company and used without further purification. ^{1}H-NMR and ^{13}C-NMR was measured on a Mercury-Plus 300 spectrometer with chemical shifts reported as ppm (in CDCl$_3$, TMS as internal standard). Mass spectra were measured with Thermo spectrometers (MAT95XP-HRMS). Fluorescence spectra were determined with a Shimadzu RF-5301PC spectrometer and the slit widths were 1.5 nm for both excitation and emission. The fluorescence spectra at low temperature were done with an Endinburgh Instruments Ltd spectrometer (FLSP920). The Differential scanning calorimetry (DSC) curves were obtained with a NETZSCH thermal analyzer (DSC 204) at a heating rate of 10 °C/min under a N$_2$ atmosphere. Thermogravimetric analyses (TGA) were performed with a TA thermal analyzer (Q50) under a N$_2$ atmosphere with a heating rate of 20 °C/min. The fluorescence quantum yield (φ_{FL}) of all the compounds in THF or THF/water mixture was evaluated using 9,10-diphenylanthracene as the reference [19].

The THF-water mixtures with different water fractions were prepared by adding Ultra-pure water slowly into the THF solution of samples under ultrasound at room temperature. For example, a 70% water fraction mixture was prepared by adding 7 mL Ultra-pure water into 3 mL of an appropriate concentration THF solution of sample in a 10-mL volumetric flask. The concentrations of all samples were adjusted to 10 μM after adding Ultra-pure water.

Cyclic voltammetry (CV) measurement was carried out on a Shanghai Chenhua electrochemical workstations CHI660C in a three-electrode cell with a Pt disk working electrode, a Ag/AgCl reference electrode, and a glassy carbon counter electrode. All CV measurements were performed under an inert argon atmosphere with supporting electrolyte of 0.1 M tetrabutylammonium perchlorate (n-Bu$_4$NClO$_4$) in dichloromethane at scan rate of 100 mV/s using ferrocene (Fc) as standard. The HOMO energy levels were obtained using the onset oxidation potential from the CV curves. The lowest unoccupied molecular orbital/highest occupied molecular orbital (LUMO/HOMO) energy gaps ΔEg for the compounds were estimated from the absorption edge of UV-vis absorption spectra. The 3,6-diiodo-9-tosyl-9H-carbazole was prepared according to the literature [20].

Synthesis of Compound P$_2$CTs

3,6-diiodo-9-tosyl-9H-carbazole (1.92 g, 3.4 mmol) and phenylboronic acid (0.90 g, 7.4 mmol) were dissolved in toluene (30 mL), and then 2 M aqueous K$_2$CO$_3$ solution (4.0 mL) and 5 drops of aliquat 336 were added. The mixture was stirred for 45 min under an argon atmosphere at room temperature. Then the Pd(PPh$_3$)$_4$ catalyst (catalytic amount) was added and the reaction mixture was stirred at 85 °C for 16 h. After cooling to room temperature, the product was concentrated and purified by silica gel column chromatography using dichloromethane/n-hexane (v/v=3/5) as eluent to yield 1.17 g of a white solid (yield 74%). ^{1}H NMR (300 MHz, CDCl$_3$) δ(ppm): 8.37(d, 2H); 8.13 (s,2H); 7.73(t,4H); 7.65(d,4H); 7.46(t,4H); 7.36(t,2H); 7.12(d,2H); 2.27(s,3H). MS (EI), m/z: 473([M]$^+$, calcd for C$_{31}$H$_{23}$NO$_2$S, 473); Anal. Calc. for C$_{31}$H$_{23}$NO$_2$S: C, 78.62; H, 4.90; N, 2.96; S, 6.77 Found: C, 78.56; H, 4.94; N, 3.01; S, 6.69.

Synthesis of the Compound P$_2$C

The P$_2$CTs (1.10 g, 2.3 mmol) was dissolved in the mixture of THF (13.8 ml) and DMSO (6.9 ml). Then H$_2$O (2.3 ml) and KOH (5.15 g, 92.0 mmol) were added and the reaction mixture was stirred at 80 °C for 4 h. After cooling to room temperature, the reaction mixture was neutralized with the solution of hydrochloric acid and a yellow solid was obtained. The crude product was purified by silica gel column chromatography using dichloromethane/n-hexane (v/v=1/1) as eluent to yield 0.70 g of a white solid (yield 95%). ^{1}H NMR (300 MHz, CDCl$_3$) δ: 8.32(s,2H); 8.11 (s,1H); 7.70(t,6H); 7.46(t,6H); 7.32(t,3H). MS (EI), m/z: 319([M]$^+$, calcd for C$_{24}$H$_{17}$N, 319); Anal. Calc. for C$_{24}$H$_{17}$N: C, 90.25; H, 5.36; N, 4.39 Found: C, 90.16; H, 5.41; N, 4.32.

Synthesis of the Compound (PBC)$_2$-PBr

A mixture of P$_2$C (1.50 g, 4.7 mmol) and Postassium tert-butoxide (1.05 g, 9.4 mmol) were stirred in DMF (20 mL) at room temperature for 30 min. Bis(4-fluorophenyl) methanone (0.46 g, 2.1 mmol) was then added to the mixture and a yellow precipitate appeared after stirring at 70 °C for 6 h. The yellow precipitate was filtrated and dried without further purification due to the slightly solubility. The crude product and diethyl-4-bromobenzylphosphonate (0.78 g, 2.5 mmol) were added to the anhydrous tetrahydrofuran (30 ml) and the mixture was stirred under a N$_2$ atmosphere at room temperature. Then the Postassium tert-butoxide (2.2 g, 20 mmol) was added quickly and the mixture was stirred continuously for 2 h. The reaction mixture was precipitated with ethanol and the crude product

was collected. Further purification can be accomplished by silica gel column chromatography with dichloromethane/n-hexane (v/v=3/5) as eluent. A yellowish green powder was abtained with a total yield of 49%. ^{1}H NMR (300 MHz, CDCl$_3$) δ: 8.40(s,4H); 7.76-7.62.(m,18H); 7.59-7.44(m,14H); 7.36(q,6H); 7.12(s,1H); 7.04(d,2H). ^{13}C NMR (125 MHz, CDCl$_3$) δ(ppm): 141.98, 141.95, 140.77, 138.97, 137.53, 137.45, 136.16, 134.05, 132.22, 131.61, 131.40, 129.30, 129.05, 128.52, 127.54, 127.43, 126.90, 125.97, 124.41, 121.47, 119.19, 110.48, 110.41. FT-IR (KBr) υ (cm^{-1}): 3029 (Ar and =C–H stretching), 1600, 1514, 1457, 1266, 815, 760, 700, 650. MS (EI), m/z: 970([M]$^+$, calcd for C$_{68}$H$_{45}$BrN$_2$, 970); Anal. Calc. for C$_{68}$H$_{45}$BrN$_2$: C, 84.20; H, 4.68; N, 2.89; Br, 8.24 Found: C, 84.16; H, 4.62; N, 2.92; Br, 8.20.

General Procedure for the Synthesis of Compounds (PBC)$_2$-TB, (PBC)$_2$-N and (PBC)$_2$-P

(PBC)$_2$-PBr (0.40, 0.4 mmol) and the corresponding boric acid (0.5 mmol) were dissolved in toluene (25 mL), and then 2 M aqueous K$_2$CO$_3$ solution (0.5 mL) and 3 drops of aliquat 336 were added. The mixture was stirred for 45 min under an argon atmosphere at room temperature. Then the Pd(Pph$_3$)$_4$ catalyst (catalytic amount) was added and the reaction mixture was stirred at 85°C for 16 h. After cooling to room temperature, the product was concentrated and purified by silica gel column chromatography using dichloromethane/n-hexane (v/v=1/2) as eluent. Yields of products: (PBC)$_2$-TB 73%; (PBC)$_2$-N 60%; (PBC)$_2$-P 54%.

(PBC)$_2$-TB

^{1}H NMR (300 MHz, CDCl$_3$) δ: 8.40(s,4H), 7.76-7.64 (m,18H); 7.64-7.54(m,8H); 7.54-7.42(m,14H); 7.34(t,4H); 7.24(s,1H); 1.36(s,9H). ^{13}C NMR (75 MHz, CDCl$_3$) δ(ppm): 150.72, 142.25, 142.03, 140.84, 140.00, 139.56, 137.68, 137.28, 135.95, 134.02, 132.34, 130.33, 129.25, 127.53, 126.87, 126.00, 124.40, 119.17, 110.46, 34.95, 31.74. FT-IR (KBr) υ (cm^{-1}): 3029 (Ar and =C–H stretching), 2962, 2866, 1600, 1512, 1457, 1264, 817, 760, 697. MS (EI), m/z: 1023([M]$^+$, calcd for C$_{78}$H$_{58}$N$_2$ 1023); Anal. Calc. for C$_{78}$H$_{58}$N$_2$: C, 91.55; H, 5.71; N, 2.74 Found: C, 91.48; H, 5.69; N, 2.66.

(PBC)$_2$-N

^{1}H NMR (300 MHz, CDCl$_3$) δ: 8.40(s,4H); 7.82-7.98 (m,3H); 7.78-7.62(q,20H); 7.59(t,5H); 7.52-7.38 (m,13H);7.38-7.26(m,7H). ^{13}C NMR (75 MHz, CDCl$_3$) δ(ppm): 142.17, 142.01, 141.20, 140.79, 139.95, 139.85, 139.54, 137.33, 136.19, 133.99, 132.36, 131.63, 130.19,

129.86, 129.53, 129.30, 129.05, 128.60, 128.02, 127.54, 127.15, 126.90, 126.38, 125.99, 125.65, 124.38, 119.19, 110.54, 110.42. FT-IR (KBr) υ (cm^{-1}): 3029 (Ar and =C–H stretching), 2961, 2866, 1607, 1497, 1459, 1260, 1113, 822. MS (FAB), m/z: 1017([M]$^+$, calcd for C$_{78}$H$_{52}$N$_2$, 1017); Anal. Calc. for C$_{78}$H$_{52}$N$_2$: C, 92.09; H, 5.15; N, 2.75 Found: C, 92.01; H, 5.12; N, 2.69.

(PBC)$_2$-P

^{1}H NMR (300 MHz, CDCl$_3$) δ: 8.40(d,4H); 8.24-8.16 (m,3H); 8.14-8.05(m,3H); 8.04-7.94(m,3H);7.80-7.62 (m,20H); 7.62-7.54(m,5H); 7.53(s,1H); 7.51-7.39(m,8H); 7.39-7.28(m,7H). ^{13}C NMR (75 MHz, CDCl$_3$) δ(ppm): 142.03, 141.93, 141.39, 140.84, 140.40, 139.59, 137.40, 137.30, 136.25, 134.03, 132.41, 131.69, 131.13, 130.88, 130.69, 129.96, 129.54, 129.30, 129.02, 128.65, 127.85, 127.71, 127.54, 127.48, 126.88, 126.26, 125.99, 125.42, 125.25, 125.13, 124.93, 124.41, 119.16, 110.53, 110.40. FT-IR (KBr) υ (cm-1): 3034 (Ar and =C–H stretching), 1600, 1512, 1457, 1269, 815, 760, 700. MS (FAB), m/z: 1091([M]$^+$, calcd for C$_{84}$H$_{54}$N$_2$, 1091); Anal. Calc. for C$_{78}$H$_{54}$N$_2$: C, 92.45; H, 4.99; N, 2.57 Found: C, 92.39; H, 4.91; N, 2.48.

Results and Discussion

Synthesis

The synthetic routes of this new series of diphenylcarbazole triphenylethylene derivatives are outlined in Scheme 1, and the chemical structures of reference compounds **5,7** and **8** are shown in Scheme 2. The modification of carbazole, as already known, is possible with high reactivity and selectivity at positions 3 and 6. The functional group benzene was selected and introduced to carbazole in consideration of its solubility, thermal stability and increase in π–π conjugation, all of which are assumed to benefit light emission enhancement. (PBC)$_2$-PBr, the key precursor, was synthesized from bis(4-(3,6-dipenyl-9H-carbazol-9-yl)phenyl) methanone [(PBC)$_2$-one] and diethyl 4-bromobenzyl-phosphonate through the Wittig-Horner reaction with a yield of 49.4% for the slight solubility of the (PBC)$_2$ -one. The desired compounds were obtained through cross-coupling of (PBC)$_2$-PBr with several aryl-boronic acids under Pd-catalyzed Suzuki reactions. The yields ranged from 54 to 73%.

The structural information of the compounds was obtained with proton nuclear magnetic resonance imaging (^{1}H NMR), carbon nuclear magnetic resonance imaging (^{13}C NMR), Fourier transform infrared spectroscopy (FT-IR), and high-resolution mass spectroscopy (MS).
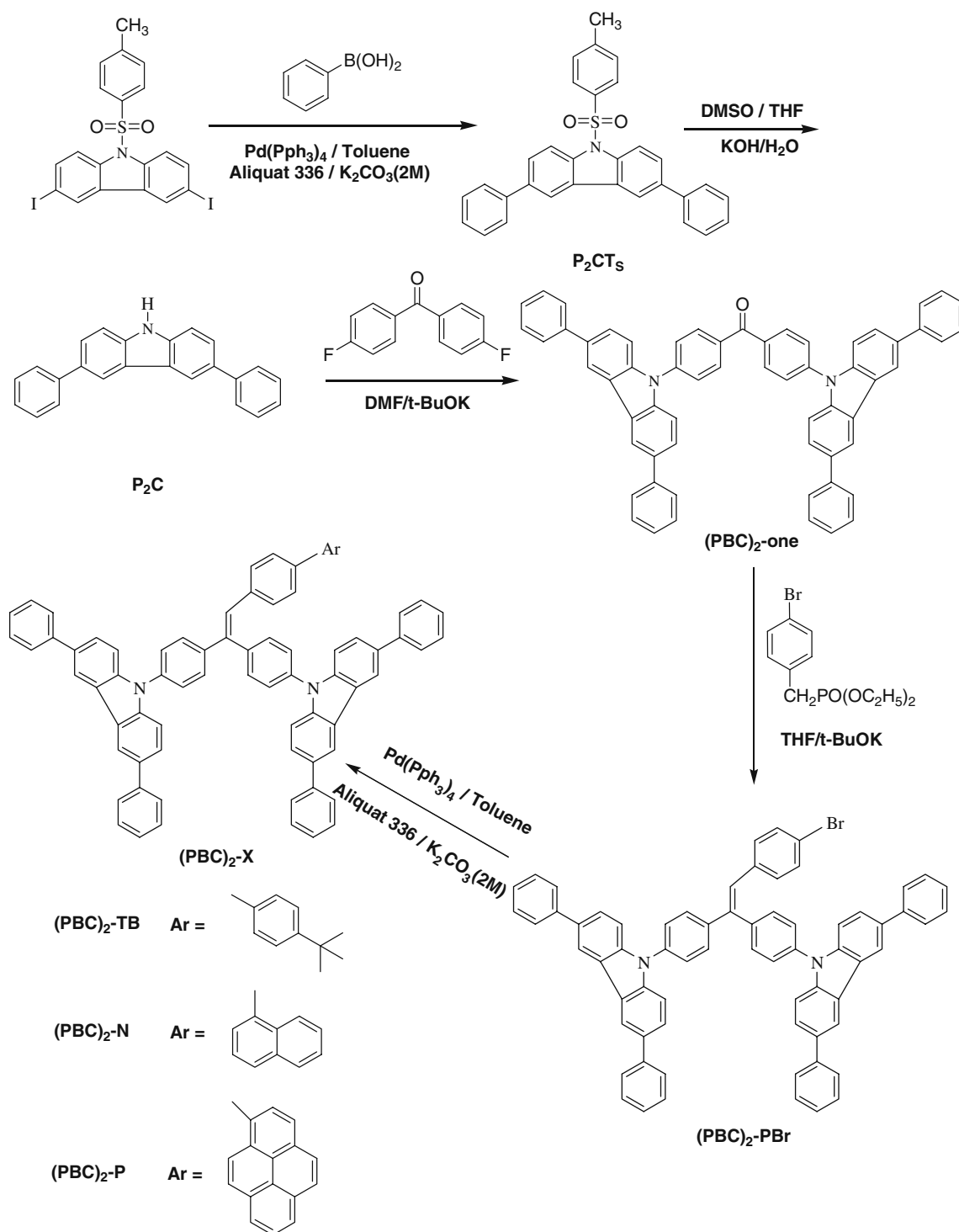
Scheme 1 Synthetic routes for the new compounds

Thermal Properties

Thermogravimetric analysis (TGA) and differential scanning calorimetry (DSC) were utilized to investigate the thermal properties of all target compounds. The test results are summarized in Table 1.

We measured the decomposition temperatures (T_d) of **(PBC)$_2$-TB**, **(PBC)$_2$-N**, and **(PBC)$_2$-P**, which were determined from the point of 5% weight loss during heating in nitrogen. These were found to be 501, 540 and 549 °C, respectively. The TGA curves of each compound are presented in Fig. 1. The figure shows that all the
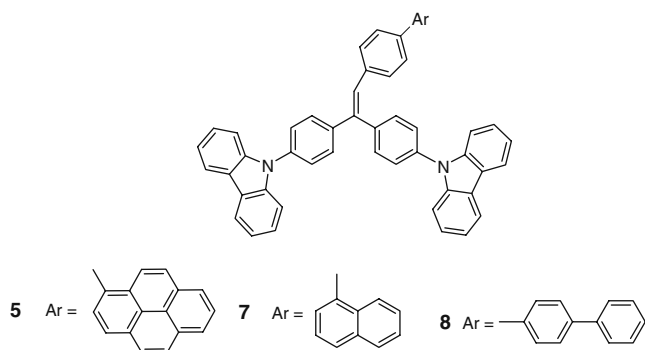
Scheme 2 The chemical structures of compounds 5,7 and 8 as references

Fig. 1 TGA curves of the compounds

compounds are highly stable. Their T_d values were much higher than MPPS (309 °C) and HPS (351 °C), both of which are typical AIE-active molecules reported in the literature [21]. They were also higher than all the triphenylethylene carbazole derivatives of compounds **4** to **8** (453 to 488 °C) [18]. Due to the substituents of benzene attached to the carbazole core, the heighten of T_d value of the derivatives approached 100 °C. **(PBC)₂-P**, which is a diphenylcarbazole triphenylethylene derivative functionalized by the fused ring of a pyrenyl group, had the highest T_d value, and **(PBC)₂-N**, which is functionalized by the fused ring of a naphthyl group, was most similar to it. In contrast, **(PBC)₂-TB**, which does not contain a fused ring, had a T_d value that was about 39 to 48 °C lower. This indicates that the introduction of a fused ring is beneficial in enhancing the thermal properties of the derivatives.

The glass transition temperatures (T_g) of the compounds were measured by DSC, and the second heating curves, running at a scan rate of 10 °C/min in a nitrogen atmosphere, are shown in Fig. 2. The results of the investigation indicate that all the compounds exhibited glass transition peaks, with T_g values ranging from 168.2 to 182.4 °C. The T_g values are about three times those of MPPS(54 °C) and HPS(65 °C) [21]. Furthermore, **(PBC)₂-N** and **(PBC)₂-P** were 45 and 31 °C higher, respectively, than the corresponding triphenylethylene carbazole derivatives of compounds **7** and **5** (126.6 and 151.1 °C, respectively). This is due to the benzene substituents attached to the carbazole core [18]. The T_g of **(PBC)₂-P** was the highest (182.4 °C), and this can be attributed to its significant increase in molecular weight and bulky pyrenyl group substituent.
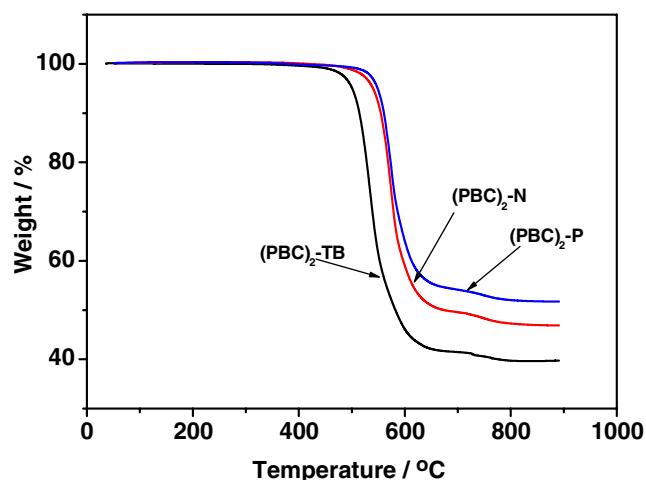
As can be seen from Fig. 2, the DSC curves of the derivatives show no crystallization or melting peaks but only glass transition peaks. The results from these thermal behaviors are expected to yield better electroluminescent properties for minimal crystal formation when cooling from the melted state.

Optical Properties

The optical properties of the diphenylcarbazole triphenylethylene derivatives were investigated both in tetrahydrofuran (THF) solution and TLC thin films at room temperature. The results of this analysis are summarized in Table 2.

The maximum absorption wavelengths of **(PBC)₂-TB**, **(PBC)₂-N** and **(PBC)₂-P** were found to be 343, 341, and 358 nm, respectively. Compared with the corresponding triphenylethylene carbazole derivatives of compounds **7**
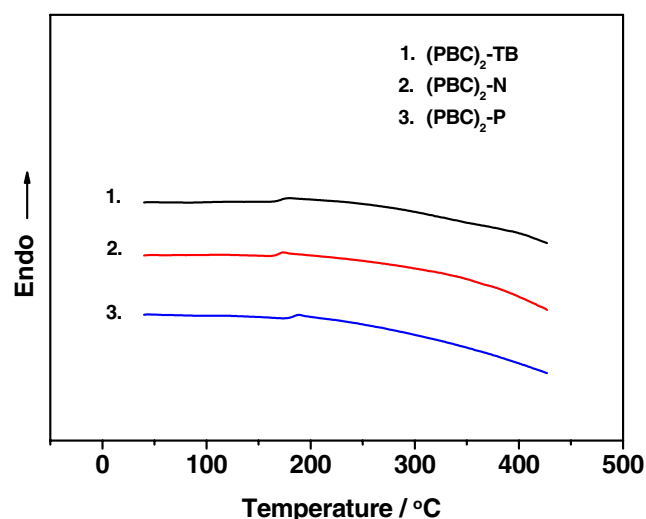
Table 1 Thermal properties of the compounds

Sample	T_g (°C)	T_m (°C)	T_d (°C)
(PBC)₂-TB	168.2	N/A	501
(PBC)₂-N	171.2	N/A	540
(PBC)₂-P	182.4	N/A	549

Fig. 2 DSC curves for the compounds at a scan rate of 10°C/min (second heating scan)

Table 2 Optical properties of the compounds

Sample	λ_{max}^{abs} (nm)	λ_{max}^{em} (nm)		ϕ_{FL} (%)	
	a	b	c	d	e
(PBC)$_2$-TB	343	465	459	2.2	40.0
(PBC)$_2$-N	341	457	450	2.1	32.2
(PBC)$_2$-P	358	466	470	8.7	69.4

[a] In THF; [b] InTHF; [c] in TLC thin film; Fluorescence quantum yields were measured in [d] THF solution and [e] cyclohexane solution using 9,10-diphenyl- anthracene as standard.

and **5** (at 343 and 360 nm, respectively), the introduction of four benzene rings to the carbazole cores did not cause the maximum absorption wavelengths of the compounds to red-shift. Rather, slight blue-shifts were found [18]. This could be attributed to the effect of the benzenes rings linked to the carbazoles. An increase in volume and enhancement of the twisted configuration could decrease the π–π conjugation of the molecule.

The photoluminescent spectra of the compounds **(PBC)$_2$-TB**, **(PBC)$_2$-N** and **(PBC)$_2$-P** in THF solution showed maxima at 465, 457, and 466 nm, respectively, while the maxima in solid thin films were found to be 459, 450 and 470 nm, respectively. These indicate that all the compounds exhibit blue light emission in both THF solution and solid thin films.

As compared to the THF solution, the compounds **(PBC)$_2$-TB** and **(PBC)$_2$-N** were blue-shifted in the case of solid thin films due to the more significantly twisted configuration of the molecules in the solid state. In contrast

and similar to the corresponding triphenylethylene carbazole derivative of compound **5** [16], the planarity of the pyrenyl group caused (PBC)$_2$-P to exhibit an opposite phenomenon, resulting in red-shift of the PL spectrum caused by the strong intermolecular interaction between the pyrenyl groups.

The quantum yields (Φ_{FL}) of all the derivatives in THF with 9,10-diphenylanthracene as standard (Φ_{FL}=90%) ranged from 2.2 to 8.7%. However, the Φ_{FL} determined in cyclohexane was in the range of 32.2 to 69.4%, 8- and 18-fold increased in Φ_{FL} when compared to those of THF solutions and cyclohexane solutions, respectively.

AIE Properties

AIE behavior is commonly proven by the emission enhancement resulting from fluorescent nanoparticle formation [10, 11, 22]. We measured the fluorescent emission of all the compounds in aqueous THF at different water/ THF ratios, and the corresponding emission spectra of **(PBC)$_2$-TB** are shown in Fig. 3. As can be seen from the figure, the PL signals of the compound in a dilute solution of THF are quite weak, and they remained almost unchanged when up to 50% (v/v) water was added. This phenomenon may be attributed to the fact that the intramolecular rotation of **(PBC)$_2$-TB**, which serves as the relaxation channel for the excited state to decay, is active [14]. When the water fraction reached 60% (v/v), however, the PL intensity was boosted to 192. The highest PL intensity value of 245 was obtained at the water fraction of 90%(v/v) while in pure THF the highest PL intensity value obtained was only 16. This dramatic enhancement in

Fig. 3 PL spectra of **(PBC)$_2$-TB** in various water/THF mixtures. The inset depicts the changes in PL peak intensity
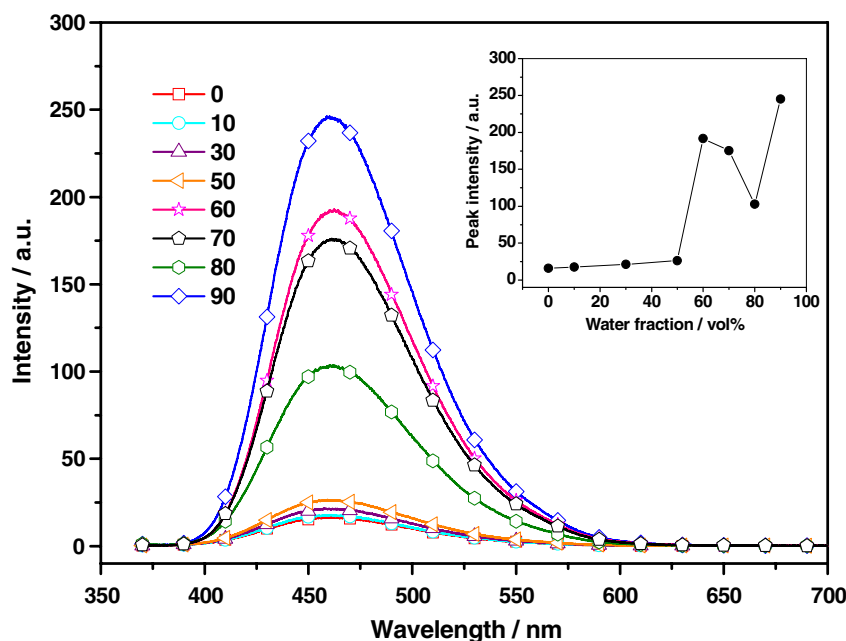
luminescence indicates that the nanoparticles are formed in the proportion of 60:10 (v/v) water/THF, and that intramolecular rotation is restricted due to physical constraint [14]. When the water fraction was higher than 60%, the PL intensity showed no regularity. We suggest this because solute molecules may aggregate into crystal and amorphous particles. The former leads to an enhancement in the intensity of photoluminescent emission, while the latter leads to its reduction. Thus, the measured photoluminescent intensity often shows no regularity for the uncontrollable formation of the nanoparticles in solutions with high water content. Similar effects were observed for the other compounds. The emission images of (PBC)$_2$-TB in pure THF, 90:10 (v/v) water/THF and a TLC solid thin film under UV light (365 nm) illumination at room temperature are shown in Fig. 4. Clearly, (PBC)$_2$-TB in both water fraction of 90%(v/v) water/THF and the solid thin film exhibited very strong fluorescence, while the same compound showed weak fluorescence in THF solution.

Different absorption behaviors are seen as the water fractions in the solutions increased. These difference were observed by investigating the UV absorption spectra of (PBC)$_2$-TB in different ratios of water and THF (Fig. 5). The absorption intensities of (PBC)$_2$-TB were virtually unchanged from water fractions of 0% to 50%(v/v) water/THF. However, when the water fraction of the water/THF mixture increased to 60% (v/v), the entire spectrum began to rise and showed a long-wavelength absorption tail. This is due to light-scattering effects in the solution, which suggests the formation of aggregates that effectively decrease light transmission through the mixtures [23]. The abrupt increase in absorbance in the 60% water fraction corresponds to the sudden jump in PL intensity and quantum yield as shown in Fig. 3 and Table 3.
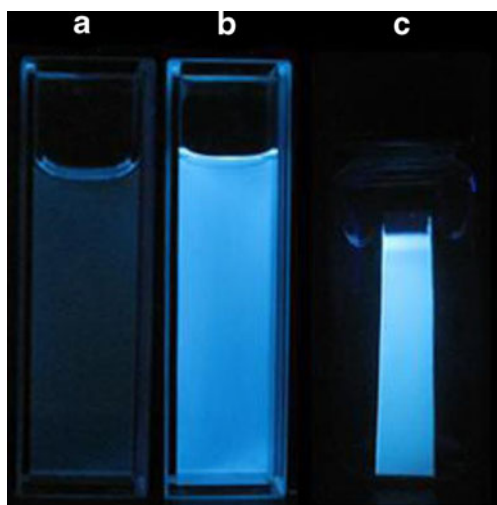

Fig. 4 Emission images of (PBC)$_2$-TB in (a) pure THF (10 μM), (b) 90% water/THF solution (v/v), and (b) TLC thin film under UV light (365 nm) illumination at room temperature
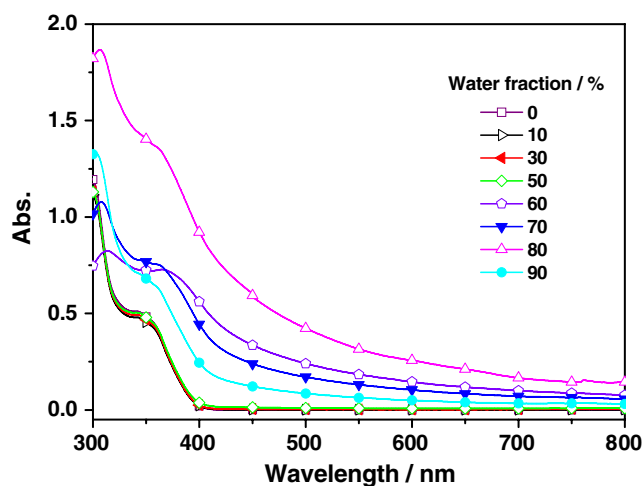

Fig. 5 UV absorption spectra of (PBC)$_2$-TB in water/THF mixtures with different volume fractions of water

The photoluminescent quantum yields (Φ_{FL}) of all compounds, estimated in different ratios of water and THF mixtures relative to 9,10-diphenyl-anthracene (DPA), are summarized in Table 3. As can be seen, the aggregates in aqueous mixtures exhibited fluorescence quantum yields ranging from 20 to 46%, which are much higher than those of the solutions in pure THF (2.0 to 8.5%). The changes in Φ_{FL} values agree well with the observed behaviors of absorption and photoluminescence, both of which showed abrupt increases when the water fraction reached 60% (v/v). Similar to the changes in PL peak intensity, the quantum yields showed no regularity when the water fraction was higher than 60%, suggesting that different and uncontrollable proportions of crystal and amorphous particles are formed in high water content solutions. The above results indicate that the compound molecules start to aggregate significantly when the volume fraction of water is around 60%. Moreover, the results prove the existence of AIE properties in all the derivatives.

The effects of temperature on the PL relative peak intensity of the compounds and DPA in dilute THF solutions (10 μM) were also investigated, and the corresponding curves are shown in Fig. 6. When the temperature increased from 77 K, the relative peak intensity of the new compounds decreased dramatically near the melting point of THF (T$_m$, ~165 K), while that of DPA

Table 3 PL quantum yields (Φ_{FL}) of the compounds in various ratios of water and THF

H$_2$O (v %)	0	10	30	50	60	70	80	90
(PBC)$_2$-TB	2.1	2.4	2.8	3.3	18	14	5.6	20
(PBC)$_2$-N	2.0	2.4	2.9	3.6	17	15	9.5	25
(PBC)$_2$-P	8.5	9.6	11	13	46	44	28	39
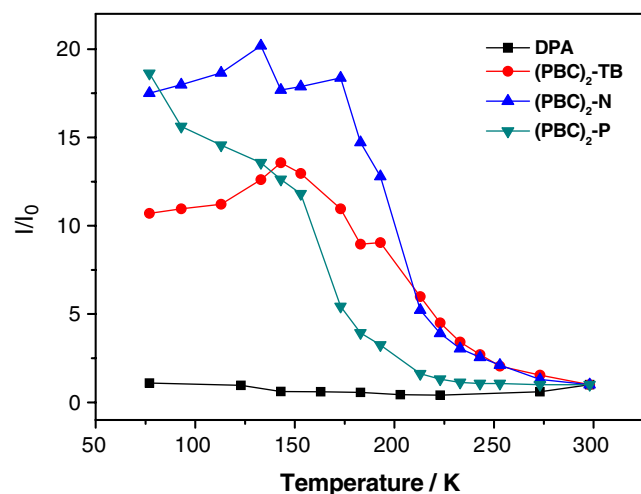
Fig. 6 Effect of temperature on the PL relative peak intensity of the new compounds and DPA in THF

Fig. 8 CV curve of (PBC)$_2$-TB in CH$_2$Cl$_2$

remained almost unchanged. This implies that when a molecule is frozen in THF, similar to the effects of aggregation in liquids, the intramolecular rotation, which serves as a relaxation channel for the excited state to decay, is blocked, and the PL intensity exhibits a dramatic increase. As compared to the carbazole triphenylethylene derivative of compound 7 [18], in which the extent of the decrease was about 40-fold and two times lager than that of (PBC)$_2$-N (20-fold), the extent of decrease seems closely related to the volume of the substituent, as smaller substituents rotate with more ease than larger ones because of smaller steric effects. From Fig. 6, it can also be seen that the extent of the decrease and the trend are not the same for
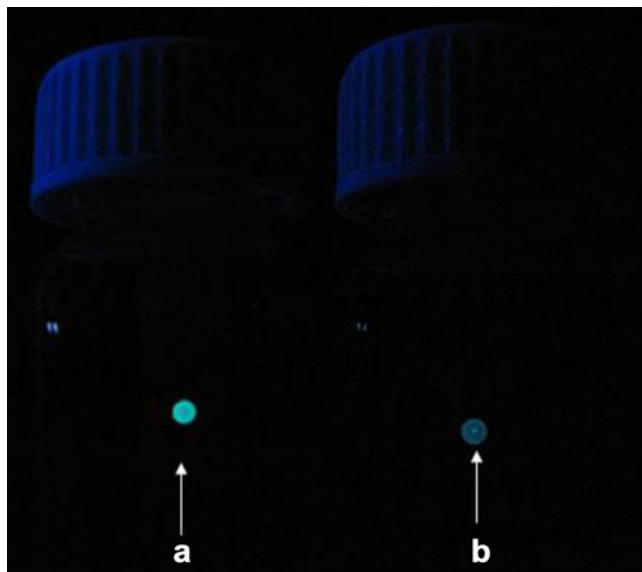
each compound. The relative peak intensity of (PBC)$_2$-P shows slow drop in all the time.

AIE materials possess the on/off fluorescence switching property in some organic vapors, it was suggested that this could be one of the most important potential applications in the photoswitch field as a chemical vapor sensor [14]. The on/off fluorescence switch effect was investigated with a spot of (PBC)$_2$-N on the thin-layer chromatography (TLC) plate (Fig. 7). Under UV light illumination (wavelength 365 nm) at room temperature, the spot showed bright blue fluorescence, which was switched off (very weak fluorescence) reversibly in an atmosphere of dichloromethane vapor. It is a probable explanation that solvation of the vapor of good solvent releases interaction of solid molecules to great extent and cause free rotation of single bonds of the AIE molecules and lead to nonemission.

Electrochemical Properties

The highest occupied molecular orbital (HOMO) and lowest unoccupied molecular orbital (LUMO) are two important parameters for electroluminescence materials due to their relationship with the hole-/electron-injecting capability of OLEDs. To test the electrochemical properties of all the derivertives, cyclic voltammetry (CV) studies were performed in CH$_2$Cl$_2$ solution, using tetrabutylammonium perchlorate (n-Bu$_4$NClO$_4$, 0.1 M) as the supporting

Fig. 7 On/off fluorescence switching of compound (PBC)$_2$-N on TLC plates without vapor (a) and in CH$_2$Cl$_2$ vapor (b) under UV light (365 nm) illumination at room temperature
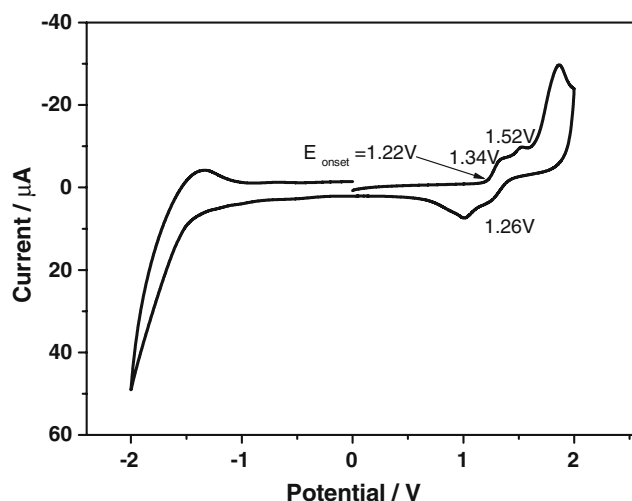
Table 4 Energy levels of the molecular orbitals and band gaps of the compounds

Sample	HOMO (eV)	LUMO (eV)	ΔEg (eV)
(PBC)$_2$-TB	5.49	2.31	3.18
(PBC)$_2$-N	5.49	2.29	3.20
(PBC)$_2$-P	5.52	2.48	3.04

electrolyte. Figure 8 shows the cyclic voltammogram of **(PBC)₂-TB**. The energy band gaps (ΔE_g) of the derivertives were estimated from the onset wavelength of their UV absorptions. The HOMO energy levels were obtained using the onset oxidation potential. The LUMO energy levels are computed from the difference between HOMO energy and the energy band gap ($\Delta E_g = \text{HOMO} - \text{LUMO}$). The HOMO, LUMO and ΔE_g values of all the compounds are listed in Table 4. The ΔE_g values of **(PBC)₂-TB**, **(PBC)₂-N** and **(PBC)₂-P** were found to be 3.18, 3.20, and 3.04 eV, respectively. The LUMO values of the compounds ranged from 2.29 to 2.31 eV, with **(PBC)₂-N** possessing the lowest and **(PBC)₂-P** possessing the highest LUMO levels. The HOMO values ranged from 5.49 to 5.52 eV. Compounds **(PBC)₂-TB** and **(PBC)₂-N** had the same HOMO level, while **(PBC)₂-P** had the highest.

Conclusions

We have synthesized a new series of diphenylcarbazole triphenylethylene derivatives, all of which are AIE active. All the compounds exhibited strong blue light emission both in the aggregated state and in TLC solid thin films. The maximum fluorescence emission wavelengths ranged from 450 to 470 nm. The derivatives exhibited excellent thermal properties, with glass transition temperatures ranging from 168.2 to 182.4 °C and decomposition temperatures (5% weight loss) ranging from 501 to 549 °C. Both of these temperature ranges are much higher than those reported in the literature for silole and carbazole triphenylethylene derivatives which were the focus of our previous work. These new derivatives are suggested as potential materials for blue light emitters in OLEDs.

References

1. Wong WWH, Holmes AB (2008) Poly(dibenzosilole)s. Adv Polym Sci 212:85–98
2. Chen J, Cao Y (2007) Silole-containing polymers:chemistry and optoelectronic properties. Macromol Rapid Commun 28:1714–1742
3. Hoeben FJM, Jonkheijm P, Meijer EW, Schenning APHJ (2005) About supramolecular assemblies of π-conjugated systems. Chem Rev 105:1491–1546
4. Bunz UHF (2000) Polyaryleneethynylenes: syntheses, properties, structures, and applications. Chem Rev 100:1605–1644
5. Kulkarni AP, Tonzola CJ, Babel A, Jenekhe SA (2004) Electron transport materials for organic light-emitting diodes. Chem Mater 16:4556–4573
6. Chen CT (2004) Evolution of red organic light-emitting diodes: materials and devices. Chem Mater 16:4389–4400
7. Thomas SW III, Joly GD, Swager TM (2007) Chemical sensors based on amplifying conjugated polymers. Chem Rev 107:1339–1386
8. Jakubiak R, Collison CJ, Wan WC, Rothberg L (1999) Aggregation quenching of luminescence in electroluminescent conjugated polymers. J Phys Chem A 103:2394–2398
9. Grell M, Bradley DDC, Ungar G, Hill J, Whitehead KS (1999) Interplay of physical structure and photophysics for a liquid crystalline polyfluorene. Macromolecules 32:5810–5817
10. Luo JD, Xie ZL, Lam JWY, Cheng L, Chen HY, Qiu CF, Kwok HS, Zhan XW, Liu YQ, Zhu DB, Tang BZ (2001) Aggregation-induced emission of 1-methyl-1,2,3,4,5-pentaphenylsilole. Chem Commun 1740–1741
11. An BK, Kwon SK, Jung SD, Park SY (2002) Enhanced emission and its switching in fluorescent organic nanoparticles. J Am Chem Soc 124:14410–14415
12. Tong H, Dong YQ, Lam JWY, Sung HHY, Williams ID, Sun JZ, Tang BZ (2006) Tunable aggregation-induced emission of diphenyldibenzofulvenes. Chem Commun 1133–1135
13. Tong H, Hong YN, Dong YQ, Häussler M, Lam JWY, Li Z, Guo ZF, Guo ZH, Tang BZ (2006) Fluorescent "light-up" bioprobes based on tetraphenylethylene derivatives with aggregation-induced emission characteristics. Chem Commun 3705–3707
14. Hong YN, Lam JWY, Tang BZ (2009) Aggregation-induced emission: phenomenon, mechanism and applications. Chem Commun 4332–4353
15. Tong H, Hong YN, Dong YQ, Häussler M, Li Z, Lam JWY, Dong YP, Sung HH Y, Williams ID, Tang BZ (2007) Protein detection and quantitation by tetraphenylethene-based fluorescent probes with aggregation-induced emission characteristics. J Phys Chem B 111:11817–11823
16. Borisov SM, Wolfbeis OS (2008) Optical biosensors. Chem Rev 108:423–461
17. Lim MH, Lippard SJ (2007) Metal-based turn-on fluorescent probes for sensing nitric oxide. Acc Chem Res 40:41–51
18. Yang ZY, Chi ZG, Yu T, Zhang XQ, Chen MN, Xu BJ, Liu SW, Zhang Y, Xu JR (2009) Triphenylethylene carbazole derivatives as a new class of AIE materials with strong blue light emission and high glass transition temperature. J Mater Chem 19:5541–5546
19. Morris JV, Mahaney MA, Huber JR (1976) Fluorescence quantum yield determinations: 9, 10-diphenylanthracene as a reference standard in different solvents. J Phys Chem 80:969–974
20. Xu T, Lu R, Liu X, Zheng X, Qiu X, Zhao Y (2007) Phosphorus (V) porphyrins with axial carbazole-based dendritic substituents. Org Lett 9:797–800
21. Ning ZJ, Chen Z, Zhang Q, Yan YL, Qian SX, Cao Y, Tian H (2007) Aggregation-induced emission (AIE)-active starburst triarylamine fluorophores as potential non-doped red emitters for organic light-emitting diodes and Cl₂ gas chemodosimeter. Adv Funct Mater 17:3799–3807
22. Levitus M, Schmieder K, Ricks H, Shimizu KD, Bunz UH, Garcia-Garibay MA (2001) Steps to demarcate the effects of chromophore aggregation and planarization in poly(phenyleneethynylene)s. 1. rotationally interrupted conjugation in the excited states of 1, 4-bis(phenylethynyl)benzene. J Am Chem Soc 123:4259–4265
23. Chen JW, Law CCW, Lam JWY, Dong YP, Lo SMF, Williams ID, Zhu DB, Tang BZ (2003) Synthesis, light emission, nanoaggregation, and restricted intramolecular rotation of 1, 1-substituted 2, 3, 4, 5-tetraphenylsiloles. Chem Mater 15:1535–1546